Revista Mexicana de Astronomía y Astrofísica, **32**, 179–192 (1996)

MODELS OF CHEMICAL EVOLUTION OF THE GALACTIC DISK: CONSIDERING DIFFERENT SFR, IMF, AND INFALL RATES

Leticia Carigi

Instituto de Astronomía
Universidad Nacional Autónoma de México, and

Centro de Investigaciones de Astronomía, Venezuela

Received 1996 June 20; accepted 1996 August 23

RESUMEN

Se presentan resultados de una serie de modelos de evolución química para el disco galáctico entre 4 kpc y 20 kpc. En particular, se estudia la influencia de diferentes formas del acrecimiento del disco y de la tasa de formación estelar sobre la distribución radial de los elementos químicos y sobre la variación radial de la densidad superficial de gas. También se han estudiado los efectos de una función inicial de masa (FIM) dependiente de la metalicidad. En los modelos la tasa de formación estelar es proporcional a una potencia de las densidades superficiales de masa del gas y de masa total (gas más estrellas), $\Psi(r,t) \propto \sigma_{gas}^{x} \sigma_{tot}^{x-1}$. El modelo que considera una FIM constante y uniforme, un acrecimiento más rápido hacia el centro y una tasa de formación estelar con $x = 1.4$, predice una distribución radial de O/H que concuerda con las observaciones de H II, pero sobrestima O/H por ~ 0.2 dex e indica una distribución más convexa que la observada. Este modelo predice una densidad superficial para la masa de gas actual cercana a las restricciones observacionales, y gradientes que se aplanan con el tiempo, en contradicción con las observaciones. Cuando el número de estrellas de muy baja masa ($m \leq 0.5\ M_{\odot}$) disminuye con la metalicidad se ajusta mejor el gradiente observado y su evolución, pero todos los modelos de este tipo no reproducen la historia química temprana de la vecindad solar.

ABSTRACT

Results from a series of chemical evolution models for the galactic disk (from 4 to 20 kpc) are presented and discussed. In particular, the influence of different forms of the infall and the star formation rate on the chemical and surface density distributions of the gaseous disk are probed. The effects of a metal-dependent initial mass function are also studied. In the models the star formation rate is proportional to a power of both, gas and total (stars plus gas) surface mass densities, $\Psi(r,t) \propto \sigma_{gas}^{x} \sigma_{tot}^{x-1}$. An $x = 1.4$ model with an initial mass function independent of time, radius or metallicity, and an infall that settles linearly faster towards the center, gives a present O/H radial distribution more convex than observed but consistent with H II observations. The model overestimates O/H by ~ 0.2 dex, and yields a present surface gas density close to the observational constraints. The model predicts chemical gradients that flatten with time, in disagreement with the observations. Models in which the relative number of very low mass stars ($m \leq 0.5\ M_{\odot}$) decreases with metallicity tend to improve the agreement with the observed gradient strength and evolution, but all models of this kind fail to reproduce the early chemical history of the solar neighborhood as derived from stellar observations.

Key words: **GALAXY–ABUNDANCES — GALAXY–EVOLUTION — ISM–ABUNDANCES — STARS–LUMINOSITY FUNCTION, MASS FUNCTION**

1. INTRODUCTION

Radial abundance gradients in our Galaxy are well established from observations of H II regions (Shaver et al. 1983; Esteban & Peimbert 1995), planetary nebulae (Faúndez-Abans & Maciel 1986; Maciel & Köppen 1994), and B-type stars (Kilian-Montenbruck, Gehren, & Nissen 1994). A substantial number of chemical evolution models try to explain these gradients, and recent models give results in good agreement with most of the observed features of the chemistry of the galactic disk.

Most recently, modelers of the chemical evolution of the Galaxy have relaxed the instantaneous recycling approximation (IRA) in their highly sophisticated codes (Tosi 1988; Matteucci & François 1989; Ferrini et al. 1994; Prantzos & Aubert 1995). Authors mostly differ on the adopted star formation rate (SFR), initial mass function (IMF), net yields from stellar nucleosynthesis, and on the details of how the galactic disk formed. In spite of all the efforts dedicated to this problem, the origin and evolution of the galactic abundance gradients is at best still poorly understood (Tosi 1996).

The shape of the low-mass end of IMF and its dependence on metallicity is still a matter of intense debate. Silk (1995) suggests that at low-metallicities, the IMF should be more biased towards formation of low-mass stars than the solar neighborhood IMF (Scalo 1986) since the protostellar mass scales as $Z^{1/5}$. In order to fit the mass-to-light ratio of M82, a starburst galaxy with metallicity just below or about solar, several authors suggest the need for an IMF with considerably lower relative number of low-mass stars than the solar neighborhood IMF (e.g., Doane & Mathews 1993; Rieke et al. 1993). On the other hand, Zinnecker (1994) argues that this conclusion depends strongly on the adopted IMF slope, and that the M/L of M82 can also be fitted with a slightly shallower than Scalo's IMF, across the whole mass range, without changing much the low-mass end of the IMF.

Recent *HST* data of Richer et al. (1995) have revealed a large number of low-mass stars $\sim 0.5\,M_\odot$ in the globular cluster M4. Also in the galactic disk, Méra, Chabrier, & Barafee (1996) argue for an excess of low-mass stars (m $< 1\ M_\odot$) at lower metallicities, but the authors do not discuss the behavior of the IMF with metallicity.

There are then several evidences of important variations of the IMF, even at a fixed metallicity, so that the IMF is not constant and homogeneous after all.

This work starts to investigate some of the possible scenarios that produce or affect chemical gradients in the galactic disk, proposed in a recent review by Peimbert (1995), in particular the effects of: a) using an IMF where the relative number of very low mass stars decreases with the oxygen abundance of the gas, b) different time-scales for the formation of the galactic disk, and c) a SFR that varies with the gas and total mass densities.

2. THEORETICAL MODEL

The chemical evolution models for the solar neighborhood of Carigi (1994) have been extended to follow the chemical history of the galactic disk between 4 kpc and 20 kpc, under the following assumptions:

1) The galactic disk originates and grows only from infall of primordial gas ($X_0 = 0.76$, $Y_0 = 0.24$), and consists of a series of independent concentric rings (2 kpc wide) without mass loss or material interchange. The ring centered at $r_\odot = 8$ kpc is labeled as the solar neighborhood.

2) The infall rate of primordial gas decreases exponentially with time, in a form suggested by Lacey & Fall (1985)

$$\dot{\sigma}_{inf} = \frac{\sigma_{tot}(r_\odot, t_g)}{(1 - e^{-t_g/\tau(r)})\,\tau(r)}\, e^{-(r-r_\odot)/R}\, e^{-t/\tau(r)}\,, \quad (1)$$

such that the accumulated total surface mass density, i.e., $\sigma_{tot}(r,t) = \int_0^t \dot{\sigma}_{inf}(r,t)\,dt$, remains exponential with respect to galactocentric distance r at all times t, and matches the present value after a time t_g. This study adopts exponential scale-lengths from $R = 3$ kpc to $R = 5$ kpc for the galactic disk (Gilmore 1989), an age of $t_g = 13$ Gyr for the galactic disk (Rana 1991), and takes $\sigma_{tot}(r_\odot, t_g) = 70\ M_\odot\ \mathrm{pc}^{-2}$ for the present observed total surface mass density in the solar neighborhood (Kuijken & Gilmore 1991).

3) The infall time scale is constant or varies linearly with radius as

$$\tau(r) = [\tau(r_\odot) - \tau(0)]\, r/r_\odot + \tau(0)\,. \quad (2)$$

In this work, models adopt different $\tau(0)$ but impose $\tau(r_\odot) = 3$ Gyr to minimize the G-dwarf problem in the solar neighborhood. In particular, the limiting case of constant $\tau(r) = 3$ Gyr is studied, but cases with $\tau(0) < \tau(r_\odot)$, for which the central regions of the disk form faster than the outskirts, are also explored.

4) The star formation rate (in $M_\odot\ \mathrm{pc}^{-2}\ \mathrm{Gyr}^{-1}$) is not only proportional to a power of the surface mass density of the gas σ_{gas}, but also to the total surface mass density σ_{tot} as suggested by Matteucci et al. (1989)

$$\Psi = \nu(r)\, \sigma_{gas}^{x}\, \sigma_{tot}^{x-1}\,. \quad (3)$$

In most models the efficiency factor $\nu(r)$ is held constant, but one case takes $\nu(r) \propto r^{-1}$ as in Prantzos & Aubert (1995). The actual normalization of ν is chosen such that the present-day $\sigma_{gas}(r_\odot, t_g)$ for the

solar neighborhood agrees with the observational estimates: $6.6 \pm 2.5\ M_\odot\ \mathrm{pc}^{-2}$ (Rana & Basu 1992), $13 \pm 3\ M_\odot\ \mathrm{pc}^{-2}$ (Kuijken & Gilmore 1989); and that at $r_\odot$ after $t = 8.5$ Gyr, all models reach the solar abundances (Grevesse & Noels 1993).

5) The mass range of the adopted IMF (Kroupa, Tout, & Gilmore 1993) is extended to cover from 0.01 to 120 $M_\odot$ (hereafter KTG IMF). Two different prescriptions for the IMF are followed: a) a metal-independent IMF and, therefore, constant in time and space (KTG IMF), and b) a metal-dependent one, IMF(x_O), explicitly dependent on the oxygen abundance by mass of the gas through an increasing factor of the relative number of very low mass stars ($m \leq 0.5\ M_\odot$) defined by Carigi et al. 1995 (see Appendix for details).

6) All stellar properties: yields, lifetimes, limiting masses for supernova explosions, and remnant masses; are dependent on initial metallicity of the progenitor gas clouds. The models do not use IRA but assume that every star ejects its envelope just after leaving the main sequence. No black holes are considered. More details on these last points as well as on the code itself can be found in Carigi (1994).

3. RESULTS

This section presents and discusses the main results from the set of models. For discussion purposes, models are arranged according to the x exponent of the star formation rate of equation (3) ($\Psi \propto \sigma_{gas}^{x} \sigma_{tot}^{x-1}$). In the following subsections three cases in particular are discussed: $x = 1$, $x = 2$, and the intermediate case $x = 1.4$ referred to as "the best model".

3.1. Models with $\Psi \propto \sigma_{gas}$

For the better understanding of the different influences of the model ingredients, the simpler $x = 1$ case of a SFR that increases linearly with the gas surface mass density ($\Psi \propto \sigma_{gas}$) is first analyzed. Models of this kind were constructed with two different scale lengths ($R = 3$ kpc and $R = 5$ kpc), three different infall time-scales ($\tau(r) = const = 3$ Gyr, $\tau(r) = 3.2 r/r_\odot - 0.2$ Gyr, and $\tau(r) = 4.8 r/r_\odot - 1.8$ Gyr), and under the KTG IMF or the IMF(x_O) (Appendix).

3.1.1. The O/H Gradient

Lacey & Fall (1985) explored this type of SFR ($x = 1$ in eq. 3) in galactic chemical models assuming IRA, a constant IMF and stellar yields independent of metallicity. They find that models with $\tau(r) = const$ and without radial flows produce no gradients. The use of a $\tau(r) \neq const$ and of an IMF and yields dependent on metallicity are explored here to produce chemical gradients without appealing to radial flows.

All $x = 1$ and $\nu = const$ models with metal-dependent stellar yields produce gradients of different strengths depending on the model assumptions. Models with $\tau = const$ produce no gradient (as can be found analytically assuming IRA). Linear $\tau(r)$ of faster infall inwards, produce moderate gradients (~ -0.034 dex kpc^{-1}). Probing models with a more extreme quadratic $\tau(r)$ do not increase the gradients significantly.

The strongest O/H gradient (~ -0.045 dex kpc^{-1} within 4 kpc $< r <$ 10 kpc) is obtained using the IMF(x_O). The gradient strength is relatively insensitive to a change in R from 3 to 5 kpc, although $\sigma_{gas}(r)$ and $\Psi(r)$ are much flatter in a $R = 5$ kpc model. In all cases, the O/H radial profile flattens out beyond $r \sim 10$ kpc.

A Prantzos & Aubert (1995) type of SFR with a $\nu(r)$ proportional to r^{-1} was also tried. The $\nu(r) \propto r^{-1}$ model of the present work reproduces their computed O/H(r) distribution as well as most of their other results. Although the O/H gradient from this model agrees with the gradient derived from B-type stars of ~ -0.021 dex kpc^{-1} (Kilian-Montenbruck et al. 1994), what one really needs to match is the O/H distribution from H II regions of a flatter gradient ~ -0.086 dex kpc^{-1} gradient for $r < 12$ kpc (Peimbert 1979; Shaver et al. 1983), and together with its outer gradient ($r > 12$ kpc) of -0.036 dex kpc^{-1} (Vílchez & Esteban 1996). Since their atmospheres can be contaminated by stellar evolution processes, B-type stars may not be the best sampler of the chemical composition of the progenitor clouds. H II regions on the other hand, offer the extra advantage of being observable at large distances. Nevertheless, the large difference between gradients derived from H II regions and B-stars remains an interesting open problem, whose solution is fundamental for the development of a successful chemical evolution model of the galactic disk.

The aim of the present investigation is to reproduce the O/H radial distribution from H II regions, and not the shallower chemical gradient from B-type stars. The models, efforts and discussion of this work would have to be modified if the later gradient is the real sampler of the cloud chemistry.

In conclusion, all of our models $\Psi \propto \sigma_{gas} (x = 1)$ predict O/H radial distributions that are flatter than observed (from H II regions). This same result of flat gradients for SFR linearly proportional to the gas density has already been emphasized by several authors, in the last decade or so. Using stellar properties dependent on metallicity and a KTG IMF (with $\tau(r) \neq const$) produces only moderate chemical gradients. Under the assumptions and construction of our present models, more pronounced gradients can only be obtained using the IMF(x_O).

3.1.2. The Chemical History of the Solar Neighborhood: Failure of the Metal-Dependent IMF(x_O)

Although an IMF(x_O) in which the relative number of very low-mass stars decreases with oxygen abundance works very well for irregular galaxies (Carigi et al. 1995), and actually improves the derived O/H gradients in the galactic disk as discussed above, it fails to reproduce the early chemical history of the solar neighborhood.

Figure 1*a* shows the time evolution of [O/H] in the solar neighborhood. Model predictions with the KTG IMF and with the IMF(x_O) are shown (thin and thick lines, respectively) together with data from G-dwarf stars observed by Edvardsson et al. (1993) between $r = 7.5$ kpc and $r = 8.5$ kpc (filled dots). The solar atmospheric O/H abundance is taken from Grevesse & Noels (1993) and, just for displaying purposes, 8.5 Gyr is adopted as the time at which the sun formed. Clearly, the IMF(x_O) predicts too low an [O/H] at early times, failing to reach the [O/H] > -0.5 of G-dwarfs a few Gyr older than the sun.

During the first 5 Gyr of the evolution ($x_O < 0.002$), the adopted IMF(x_O) assigns fewer massive stars than the KTG IMF (by factors of 2 to 5). These stars are important contributors of oxygen, and therefore [O/H] $= -0.5$ is reached after ~ 6 Gyr, much later than in the model with the constant IMF. Solar abundance is reached at the right time (8.5 Gyr) because the IMF(x_O) produces 1.5 as many of these stars as the KTG IMF during the last 6.3 Gyr of evolution ($x_O > 0.004$).

Figure 1*a* shows the [C/O] abundance ratio as a function of [O/H] for the solar neighborhood. Model predictions are marked by the continuous lines as before. The filled squares mark observations of solar-neighborhood F and G dwarfs from Clegg, Lambert, & Tomkin (1981). The enclosed area represents data from Abia, Canal, & Isern (1991) modified according to Bessell, Sutherland, & Ruan (1991) who argue that oxygen abundances from the [O I] triplet overestimate the O abundance, by about a factor of four, relative to derivations from the [O I] 6300 and OH lines which originate in the same zone where lines from heavy metals form. Therefore, in Figure 1*b* the oxygen abundances from Abia et al. (1991) have been shifted down by 0.6 dex. The solar C/H abundance is also taken from Grevesse & Noels (1993).

At very early times (when [O/H] < -2 dex or $t < 0.5$ Gyr), the [C/O] predicted with the IMF(x_O) is ~ 0.2 dex higher than with the KTG IMF. Massive stars eject much less C than O at low metallicities, so the early carbon enrichment is less affected by the relative number of massive stars at early times. Since at low [O/H] the IMF(x_O) assigns fewer massive stars than the KTG IMF, the IMF(x_O) model predicts a higher [C/O] at the onset of the evolution (Figure 1*b*). This C/O offset between the models is eventually overcome since: 1) the C/O relative yield from Maeder (1992) increases strongly with metallicity; 2) the relative number of stars more massive than 0.5 $M_\odot$ increases with metallicity (and therefore their net chemical yield) in an IMF(x_O) but remain constant in the KTG IMF; and 3) the C/O relative contribution from low-and-intermediate-mass stars ($0.8 \leq m/M_\odot \leq 7.5$, hereafter LIMS) becomes more important at later times.

One could attempt to increase the early O/H enrichment of the IMF(x_O) models with a stronger SFR via a faster infall ($\tau < 3$ Gyr), but even very fast infalls do not reach the observed [O/H] of old stars fast enough. This is because a lower τ (eq. 1) requires a lower normalization of the SFR (ν in eq. 3) to match the present gas consumption at the right time.

As a first try to measure the dependence of the results with the adopted yields, the Maeder (1992) yields at solar-metallicity were substituted with those of Weaver & Woosley (1993), but keeping Maeder's yields for $Z = 0.001$ (see the Appendix for details). Under this construction, differences with the previous model become important only after reaching [O/H]> -0.3. The model with the later yields (not shown), with a small dependency on the assumed IMF, predicts at late times an [O/H] higher by ~ 0.1–0.2 dex than the previous models of Figure 1*a*. Since Weaver & Woosley (1993) predict lower C/O yields, the late evolution ([O/H]> -0.3) of [C/O] flattens out with respect to the previous models, better fitting the data shown in Figure 1*b*.

In conclusion, the IMF(x_O) with a metal-free infall fails to reproduce the early chemical history of the solar neighborhood regardless of the solar-metallicity yields or the infall rates adopted. In the following sections models with non-linear SFR ($x \neq 1$ in eq. 3) are presented and discussed, but unfortunately, with very similar results on the early chemical history of the solar neighborhood. In a future work, other yields and SFR forms will be explored, as well as different IMF dependencies with metallicity, to better reproduce the chemistry of the solar neighborhood, the galactic gradients and their evolution, as well as the chemical composition of irregular galaxies.

3.2. Models with $\Psi \propto \sigma_{gas}^2\ \sigma_{tot}$

The previous section showed that to reproduce the observed gradients from H II regions, a stronger than $x = 1$ dependency of the SFR on surface mass density is needed. In this section the use of an $x = 2$ SFR (eq. 3), i.e., $\Psi = \nu\, \sigma_{gas}^2 \sigma_{tot}$ is explored.

Matteucci et al. (1989, MFFT) also studied the $x = 2$ case but with metal-independent stellar properties. When using their $r_\odot = 10$ kpc instead of $r_\odot = 8$ kpc adopted here, our modeling predicts basically the same present-day $\sigma_{gas}(r)$ than MFFT, but there are significant differences in the O/H abundances. MFFT predict an O/H gradient of ~ -0.094 dex

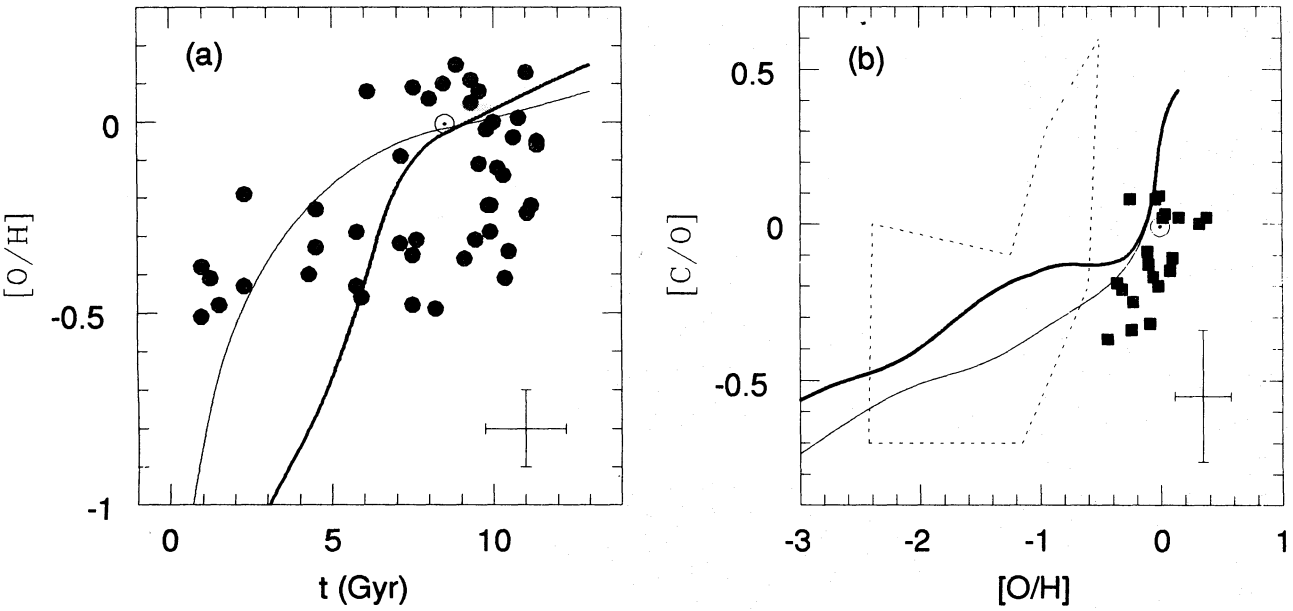

Fig. 1. The O and C abundance evolution of the solar neighborhood. Continuous lines present the predictions of $\Psi \propto \sigma_{gas}$ models with the KTG IMF (*thin lines*) and with the IMF(x_O) (*thick lines*). *(a)* [O/H] evolution. *(b)* [C/O] versus [O/H] evolution. Observational data are as follows: *circles:* Edvardsson et al. (1993); *squares:* Clegg et al. (1981). The enclosed area marks data from Abia et al. (1991) modified according Bessell et al. (1991) (see text). Crosses show typical observational errors. ⊙ marks the solar value from Grevesse & Noels (1993).

kpc^{-1} while when using a similar $\tau(r)$ our model predicts the much shallower gradient of -0.033 dex kpc^{-1} . These differences arise from the use of metal-dependent stellar properties in our modeling, and to a lesser extent to the different present-day mass distributions and IMF's assumed in both works.

Table 1 summarizes the input parameters of our set of $x = 2$ models. After the ID number, columns (2)–(5) present the adopted IMF, efficiency for SFR, scale-length of the total mass profile, and e-folding time-scale of the infall, respectively.

Figure 2 presents the radial distributions of the O/H abundance, the σ_{gas}, and the SFR predicted by the models in Table 1. O/H data from H II region observations of Peimbert (1979), Shaver et al. (1983), and Vílchez & Esteban (1996) are also plotted in panel (a). The shape of σ_{gas}(r) of Dame (1993) have been normalized to the solar neighborhood estimates of Rana & Basu (1992) and Kuijken & Gilmore (1989), of 6.6 $M_\odot$ pc^{-2} and 13.0 $M_\odot$ pc^{-2}, respectively (dotted lines in panel b). The collected data by Prantzos & Aubert (1995) for SFR radial distributions are shown in panel (c). All data have been corrected to $r_\odot = 8$ kpc.

Comparison of the first three models show that while in the external parts results are quite insensitive to the infall time-scale $\tau(r)$, towards the center the O/H radial distribution responds a little more

TABLE 1

INPUT PARAMETERS OF $x = 2$ MODELS

Model	IMF	ν ($M_\odot^{-2}$ pc^4 Gyr^{-1})	R (kpc)	$\tau(r)$ (Gyr)
1	KTG	3.0×10^{-4}	3	$4.8r/r_\odot - 1.8$
2	KTG	3.0×10^{-4}	3	$3.2r/r_\odot - 0.2$
3	KTG	3.0×10^{-4}	3	3
4	KTG	3.0×10^{-4}	5	$3.2r/r_\odot - 0.2$
5	IMF(x_O)	6.0×10^{-4}	3	$4.8r/r_\odot - 1.8$

to the slope of the adopted $\tau(r)$, as the central parts form and consume gas faster and faster than the outskirts. All but the third model, predict a similar σ_{gas}(r) beyond $\sim$ 14 kpc because the SFR and the infall rate are so low out there that the evolution of the gas density is basically governed by the shape of the infall profile.

Within $r < 11$ kpc, the results are a bit insensitive to a change of the disk scale-length from $R = 3$ kpc to $R = 5$ kpc (models 2 and 4), but not so in the outer regions due to their lower and slower gas con-

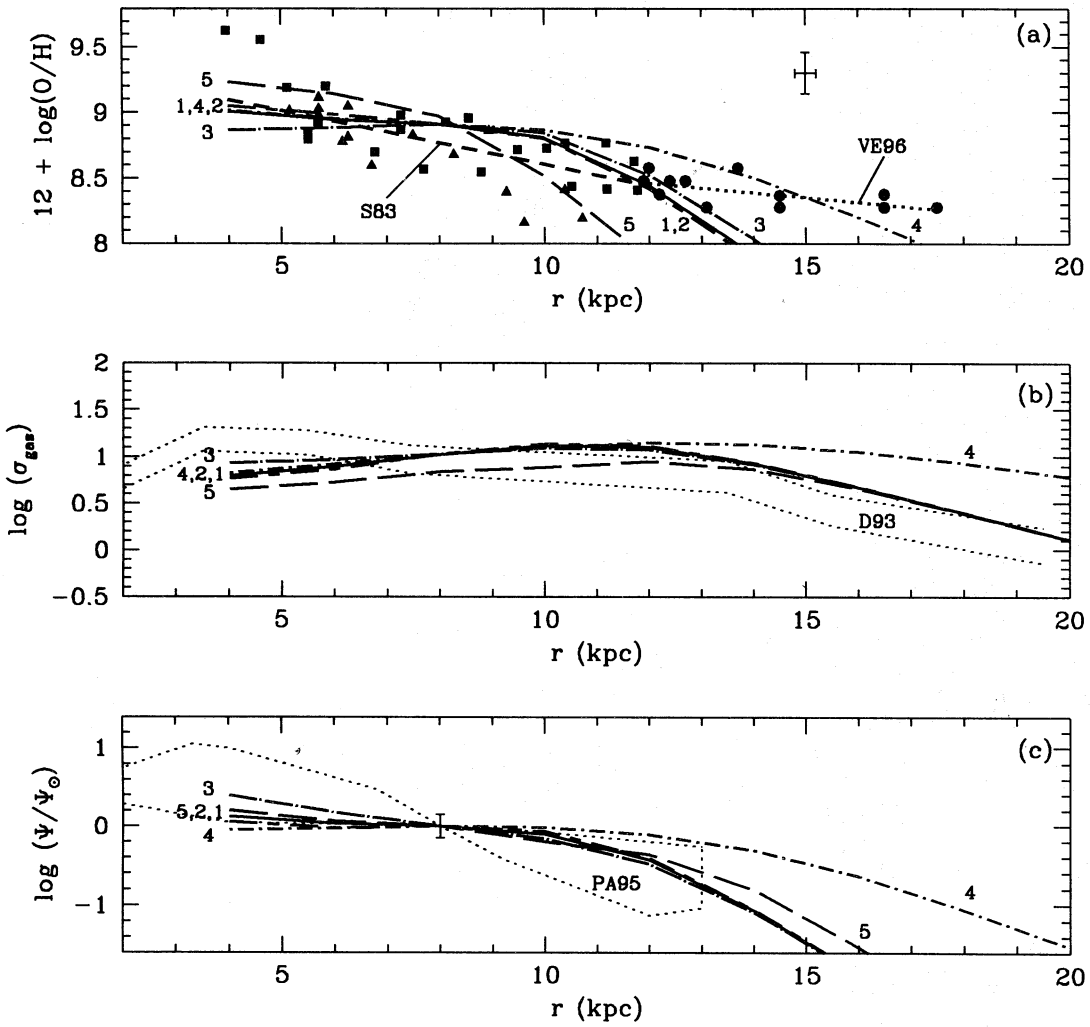

Fig. 2. The present-day radial distributions of [O/H] *(a)*, gas surface mass density *(b)* and SFR *(c)* in the galactic disk. Predictions from the five $\Psi \propto \sigma_{gas}^2 \sigma_{tot}$ models in Table 1 are marked as follows: *long-short-dash lines:* model 1; *continuous lines:* model 2; *long-dash-dot lines:* model 3; *short-dash-dot lines:* model 4; *long-dashed lines:* model 5. [O/H] observations in *(a)* are marked as follows: *squares:* Shaver et al. (1983); *triangles:* Peimbert (1979); *circles:* Vílchez & Esteban (1996). *Dashed* and *dotted lines* show the gradients suggested by Shaver et al. (1983) (S83) and by Vílchez & Esteban (1996) (Case B) (VE96), respectively. Assuming that 20% of the oxygen is locked in dust, 0.08 dex have been added to the observed [O/H] from the sources. A cross shows typical errors of the data sample. The observed gas profile in *(b)* (D93) is taken from Dame (1993) normalized to the $\sigma_{gas}(r_\odot)$ of Rana & Basu (1992) and Kuijken & Gilmore (1989) (see text). The area enclosed by dotted lines in *(c)* (PA95) indicates the data collected by Prantzos & Aubert (1995).

sumption. Nonetheless, the $R = 5$ kpc models can actually be discarded because they predict too high a present $\sigma_{gas}(r)$ at large radii (Figure 2*b*).

The IMF(x_O) (model 5) produces the strongest O/H gradient of all models (~ -0.065 dex kpc^{-1} , for 4 kpc $< r < r_\odot$) and agrees well with the observed O/H distribution from H II regions within 10 kpc, but not so beyond $\sim$ 12 kpc. For $r < 12$ kpc, this model predicts a lower present-day gas density than the rest of the models by $\sim$ 0.2 dex. The IMF(x_O) reduces the ISM enrichment, therefore it requires a more efficient SFR (higher ν in eq. 3) in order to reach solar abundances at 8.5 Gyr without consuming too much gas below the observational limit for $\sigma_{gas}(r_\odot, t_g)$.

While the O/H gradient of the model with the IMF(x_O) steepens considerably ($\sim$ 55%) respect to models with the KTG IMF, the C/H gradient (not-shown), becomes even stronger since both, the adopted C/O yields from massive stars and the relative number of these stars increase with metallicity.

Finally, like the KTG IMF model with $\Psi \propto$

σ_{gas}(§ *3.1.*), models with $x = 2$ (models 1 to 4 in Table 1) reproduce well the chemical history of the solar neighborhood. A deeper discussion on these last points is presented in § *3.3.2.* But then again, the IMF(x_O) of model 5 fails to match the high oxygen abundance of solar neighborhood G-dwarfs at early times.

3.3. The Best Model: $\Psi \propto \sigma_{gas}^{1.4}\, \sigma_{tot}^{0.4}$

In the previous sections our experiments with either a star formation rate linear on the gas surface mass density, or a SFR proportional to $\sigma_{gas}^2 \sigma_{tot}$ ($x = 1$ and $x = 2$ in eq. 3) were discussed. In the first case, the derived O/H radial distribution was shallower than observed, and in the second case the shape of the O/H distribution was not optimal (too curved). Therefore, different SFR dependencies with $1 < x < 2$ were probed to look for a better match to the observed O/H radial distribution in the galactic disk (as derived from H II regions), the gas surface mass density distribution as well as other observational constraints.

After a long series of models, our efforts converged to a "best model" characterized by $\Psi(r,t) = 0.019\, \sigma_{gas}^{1.4}(r,t)\, \sigma_{tot}^{0.4}(r,t)$, that is a SFR with $x = 1.4$ similar to the $x = 1.475$ suggested by Franco & Shore (1984), according to Matteucci et al. (1989). The best model takes a linear infall time-scale of $\tau(r) = 4.8 r/r_\odot - 1.8$ Gyr, a scale-length of $R = 3$ kpc and the KTG IMF.

3.3.1. The O/H Gradient from the Best Model

Figure 3 presents the predictions for the O/H, σ_{gas}, and SFR radial distributions from the best

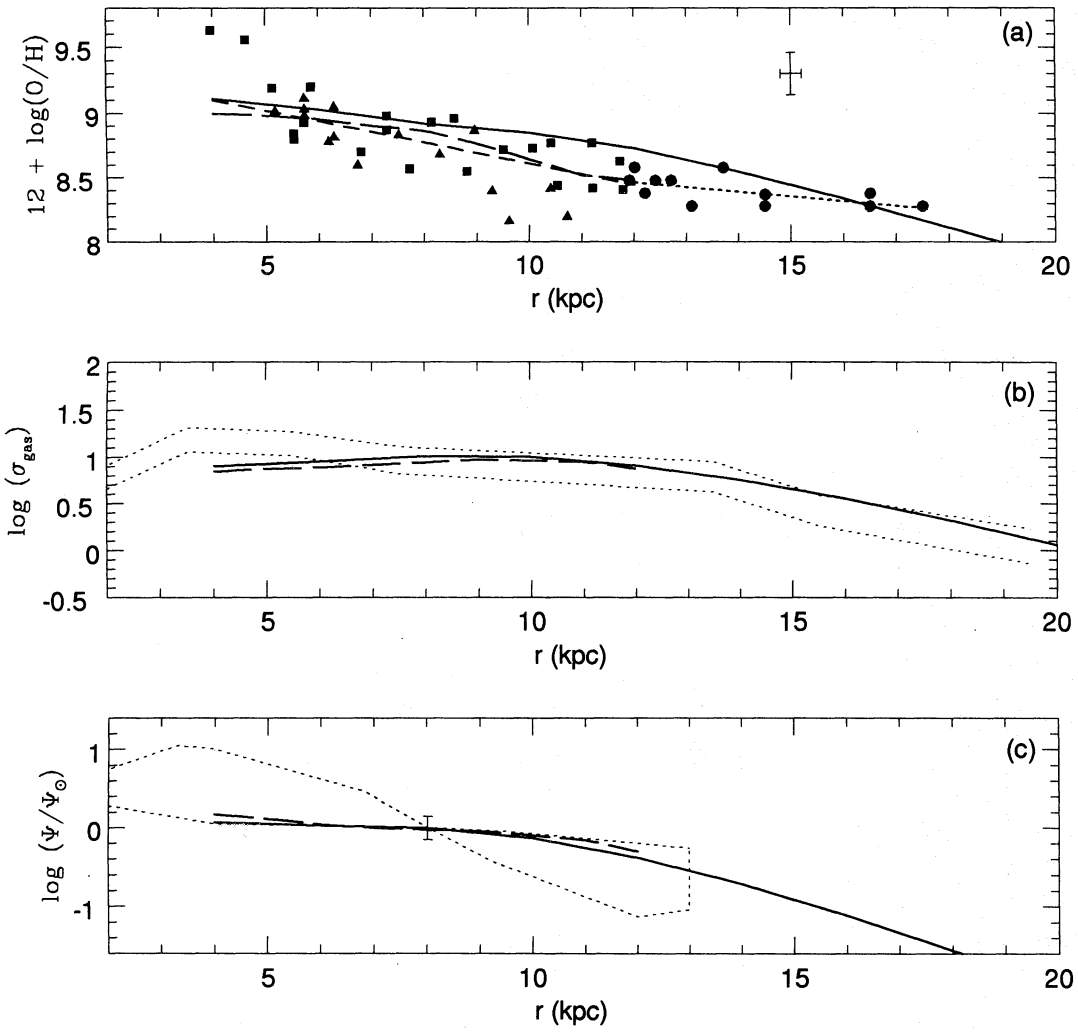

Fig. 3. Present-day radial distributions from the "best model" ($\Psi \propto \sigma_{gas}^{1.4}\, \sigma_{tot}^{0.4}$) and the relationships predicted by Ferrini et al. (1994) (*long-dashed lines*). Observational data are as in Figure 2.

model (data and symbols are as for $x = 2$ models in Figure 2). The O/H profile from this later model (thick line) is consistent with the observed distribution from H II regions, but it overestimates O/H by ~ 0.2 dex and shows too much of a convex behavior. These discrepancies cannot be removed easily without breaking the observational limits of the gas consumption (Figure 3*b*). They actually arise from the fast chemical saturation induced by the strong metallicity dependence of the oxygen yields from massive stars of Maeder (1992), which decrease strongly with metallicity. Other elements like C do not saturate as fast, and show better gradient shapes, because C yields increase with metallicity (see below). In accordance with our results, Giovagnoli & Tosi (1995) when they assume Maeder's yields also find a flattening of the O/H(r) distribution between 8 and 10 kpc ($Z < 0.02$).

The present-day surface mass density of the best model lies within the observational limits (Figure 3*b*), reaching the maximum allowed value at $r \simeq 10$ kpc. The model required maximum gas consumption towards the center ($r < 6$ kpc) to obtain the highest possible O/H central abundance (and steepest gradient) that reflected on a lower present-day SFR, $\Psi/\Psi_{\odot}(r < 8$ kpc) (Figure 3*c*) that lies at the lower limit of the observational estimates.

Figure 3 also shows the results of model A of Ferrini et al. (1994) (long-dash lines). This model assumes a slightly different IMF, other stellar yields, and a constant $\tau(r)$. These authors use a non-analytical SFR that attempts to include a variety of physical processes in the gas that should influence the star formation efficiency. The analytical SFR of our best model (Figure 3*c*) reproduces well the results from the more sophisticated treatment of Ferrini et al. (1994). The radial distributions $\sigma_{gas}(r, t_g)$ from both models are also consistent with each other (Figure 3*b*).

In the model, $\sigma_{gas}/\sigma_{tot}$ increases while σ_{inf}/Ψ decreases with galactocentric distance. This is true at all times, and in particular is consistent with the observed present-day distributions. Finally, the derived integrated infall from 4 to 20 kpc of 0.24 $M_{\odot}$ yr^{-1} of the best model lies within the observational range of $0.2 - 0.5$ $M_{\odot}$ yr^{-1} estimated by Mirabel (1989) from high velocity H I clouds.

Since Maeder's oxygen yields are particularly dependent on metallicity, while the yields used by Ferrini et al. (1994) are instead metallicity independent, the O/H gradients of their model A differ significantly from the gradients of our best model, mainly in regions with metallicities lower than solar metallicity, ($r > 9$ kpc), (Figure 3*a*).

Considering our experimentation and the work in the literature, several improvements to the models can be attempted to better reproduce the behavior of the O/H gradient in our Galaxy. In particular, one can try yields not as strongly Z-dependent as Maeder's stellar yields (eg., Woosley & Weaver 1995). Also, the addition to our modeling of an infall from a previously evolved halo could also help to explain the observed flattening of the disk's O/H gradient beyond 12 kpc.

Experience from outer galaxies is also important and should be taken into account. Edmunds & Roy (1993) and Zaritsky, Kennicutt, & Huchra (1994) find that the presence of a bar is associated with flatter abundance gradients in disk galaxies. There is evidence that our Galaxy is a barred one, and the complex distribution and kinematics of the cold gas in the galactic center ($r < 1.5$ kpc) can be understood as the inwards motion of the molecular gas induced by a rapidly rotating barred potential (Gerhard 1994). Finally, the steepening of the abundance distributions towards the center observed in our Galaxy is also common in other spiral galaxies (Díaz 1989). In conclusion, a final successful model of the galactic chemistry may have to wait for a better understanding on the formation process of the disk and on the nature and relative importance of vertical and radial material flows in our Galaxy.

3.3.2. The Solar Neighborhood from the Best Model

Figure 4 presents the detailed chemical history of the solar neighborhood with the predictions of our best model ($x = 1.4$) and the previous models of § *3.2.* ($x = 1$) and § *3.2.* ($x = 2$). The model reproduce well the enrichment histories for oxygen, iron and carbon, as well as for their relative abundances (panels a) to e) in the figure). The $x = 1.4$ SFR delays the chemical early enrichment by ~ 0.8 Gyr with respect to the $x = 1$ SFR case (Figures 4*a* and 4*b*), nearly as much as the $x = 2$ model. After ~ 4 Gyr all models show a similar behavior. The three models are consistent with the observed evolution of the relative [C/Fe] and [O/Fe] with [Fe/H] (Figures 4*c* and 4*d*).

The slope of the [O/H](t) (Figure 4*a*) basically traces the time evolution of the SFR, and therefore its dependence with the x exponent of eq. (3). During the first 3 Gyr, the SFR is more efficient the higher the x exponent. This behavior reverts itself for the next 4 Gyr or so and, at the end of the evolution the SFR of higher x models drops again, below the lower-x models, since after a time t_g all models have to consume about the same amount of gas to match the present σ_{gas}.

The early production of Fe, before supernovae of type Ia become important ($t < 1$ Gyr), is much lower than the oxygen and carbon production (mostly from SNII) in the $x = 1$ model because, as mentioned before, this SFR is more efficient at the beginning of the evolution than higher-x SFRs.

The switch over from a SNII-dominated to a SNIa-

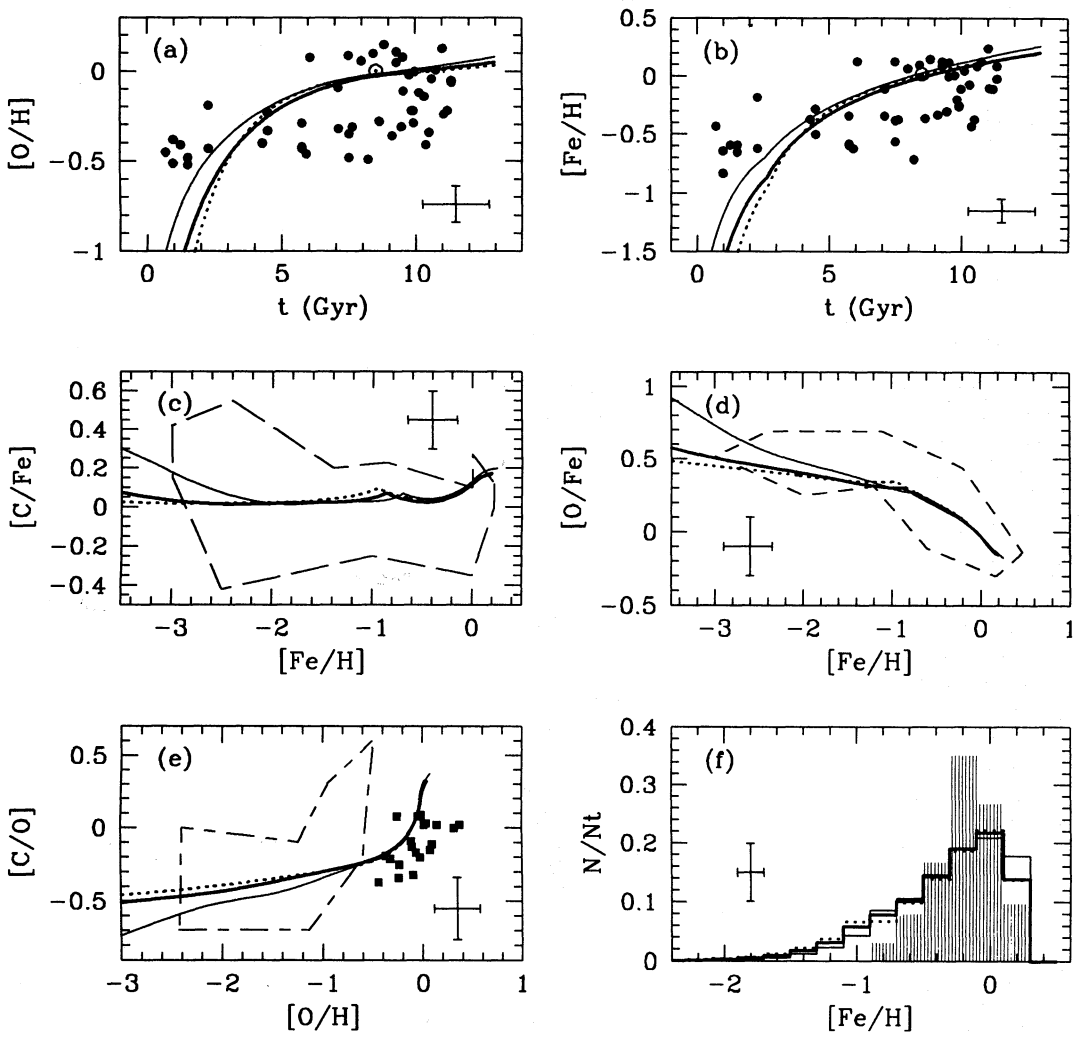

Fig. 4. Model predictions for the solar neighborhood: the best model (*thick lines*), the model with $\Psi \propto \sigma_{gas}$ (*thin lines*) and a $\Psi \propto \sigma_{gas}^2\, \sigma_{tot}$ model (*dotted lines*). *(a)* [O/H] time evolution. *(b)* [Fe/H] time evolution (data from Edvardsson et al. 1993). *(c)* [C/Fe] versus [Fe/H] evolution. *(d)* [O/Fe] versus [Fe/H] evolution. *(e)* [C/O] versus [O/H] evolution. *(f)* Normalized [Fe/H] distribution of solar neighborhood G-dwarfs. Data in *(a)*, *(b)*, and *(e)* are as in Figure 1. The enclosed areas in *(c)* and *(d)* mark the data from Abia et al. (1991), but in *(d)* the O abundance is corrected as in Figure 1. In *(f)*, *Shaded histogram* shows the stellar metallicity distribution observed by Rocha-Pinto & Maciel (1996). Crosses show typical observational errors.

dominated Fe production occurs at almost the same time for all three x-dependencies of the SFR (seen as the sudden change in slope at $\sim$ 2–3 Gyr in Figure 4*b*), but show up at different [Fe/H] ratios (Figures 4*c* and 4*e*) due to the faster enrichment of models with a lower-x SFR.

The predicted G-dwarf distributions (Figure 4*f*) peak at a higher [Fe/H (by $\sim$ 0.2 dex) than the observed distribution of Rocha-Pinto & Maciel (1996). The difference cannot be overcome with a faster infall ($\tau(r_\odot) < 3$ Gyr) without exacerbating the G-dwarf problem of predicting too many low-metallicity stars. A better match with the observed distribution may be obtained with a different kind of IMF(x_O) in combination with stellar yields less dependent on metallicity (eg., Woosley & Weaver 1995) and probably some kind of pre-enrichment of the infalling gas. These possibilities are now being explored and will be discussed in the next paper of the series (Carigi & Peimbert 1997, in preparation).

3.4. Evolution of the Chemical Gradients

Figure 5 presents the He/H, C/H, O/H, and Fe/H radial distributions from the best model at four dif-

ferent times: 0.5, 4.5, 8.5, and 13 Gyr. Gradients evolve faster towards the center, and all but the He/H gradient (see below) flatten out with time as the galactic disk chemically saturates faster in the central parts and more slowly at the outskirts.

The central infall is both quick and strong, so the SFR in the inner zones is most important early in the evolution. At later epochs, the σ_{gas} is almost all exhausted and the chemical enrichment of the ISM by the late stellar populations becomes negligible. Maximum central abundances are reached relatively fast, after $\sim$ 2–6 Gyr, depending on the atomic species. The slower and lower infall at larger radii delays the chemical saturation and gas consumption in the external parts of the disk, slowing down their C, O, and Fe enrichment as these gradients flatten out with time.

The abundance radial distribution of each atomic species and its evolution responds to the particular mass and metallicity sensitivity of the yields of the specific element. In a nutshell, the characteristics of Maeder's He, O and C yields, relevant to interpret the gradient evolution from our models can be summarized as follows:

1) The oxygen yield from LIMS is negligible while the yield from massive stars decreases with metallicity Z. 2) The helium yield from massive stars increases with Z while the yield from LIMS decreases slightly with Z. 3) The carbon yield from massive stars and from low-mass LIMS ($0.8 < m/M_{\odot} < 5$) increases with metallicity. The C yield from high mass LIMS ($5 < m/M_{\odot} < 7.5$) decreases with Z. 4) The contribution of massive stars relative to LIMS is much more important in the yield of He than in those of C, mainly so at high metallicities.

At early times, the H and He gradients are flat since in our model the disk forms just from infall of H and He and there is no radial dependence of these elements in the infall. On the other hand, the first stellar generations implant the shape of the SFR to the early radial distributions of oxygen and carbon (and the rest of the metals).

In the outer zones, the carbon and oxygen distributions evolve in a similar fashion because these zones are far from saturation. The relative C/O yield increases very fast with metallicity, so the maximum possible abundance is reached faster for O than for C (at a fixed gas consumption). Therefore, while the external C/H and O/H gradients are similar for a long time, the contrast with the central abundance is more pronounced for C than O, producing a flatter O/H radial distribution than the C/H one (Figures 5*a* and 5*b*).

Although the net He stellar yield is always positive, the infall continuously dilutes it and the central He abundance only increases by $\sim$ 0.5 dex during the whole evolution (while O and C increase by orders of magnitude). Therefore, the He/H gradient remains quite flat while the He abundance slowly increases towards the center (Figure 5*c*). Saturation effects on the He abundance are not seen because helium saturates more slowly than carbon since the LIMS and high-metallicity massive stars keep producing more He than C.

The computed O/H gradients from our models flatten up with time (Figure 5*a*). This result disagrees with the observational evidence of chemical gradients derived from objects with different mean ages: H II regions (Shaver et al. 1983), the intermediate age type II planetaries ($\sim$ 5 Gyr) and the older ($\sim$ 9 Gyr) type II planetaries (Maciel & Köppen 1994), which are also shown in the figure.

The infall is stronger and gets consumed faster towards the center, therefore in our models the chemical saturation is quickly reached at the central parts, reducing the gradients with time. Ferrini et al. (1994), who use a similar infall law than here, also derive gradients that flatten up with the evolution. Chiappini, Matteucci, & Gratton (1996) on the other hand, obtain an O/H radial distribution that steepens with time with a two-stage infall model. Tosi (1996) gets a similar behavior with a constant and uniform infall, but assuming a variable and very different relation between the gas density and the SFR than eq. (3).

The use of the IMF($x_{\rm O}$) in the best model instead of the constant KTG IMF, delays the chemical saturation and gives gradients that steepen with time (within 6 kpc $< r <$ 10 kpc), but as discussed before, this IMF($x_{\rm O}$) fails to match the early abundances in the solar neighborhood.

It seems clear to us that a main limitation of the present models resides in the lack of a realistic infall law that incorporates the true dynamical history of the formation of the galactic disk. This kind of models may be successful in matching all: the strength and evolution of the galactic chemical gradients, the chemical evolution of the solar neighborhood and the chemical history of irregular galaxies with a consistent set of assumptions for the IMF and SFR.

This work has probed some of the suggestions of Peimbert (1995) to produce chemical gradients and has verified that the following are all important factors to create chemical gradients similar in magnitude to the ones observed in the galactic disk: a) yields that increase with metallicity (like Maeder's carbon yields); b) a higher fraction of massive stars with increasing metallicity from an IMF that varies with the abundance of heavy elements; c) a steeper $\sigma_{gas}/\sigma_{tot}$ distribution with r; and d) a $\dot{\sigma}_{inf}/\Psi$ that increases with r. Nevertheless, none of these factors can explain that gradients increase with time, with the possible exception of an adequate metal-dependent IMF($x_{\rm O}$).

The existence of radial flows of gas, outwards at $t < 4$ Gyr and inwards for the rest of the disk's evo-

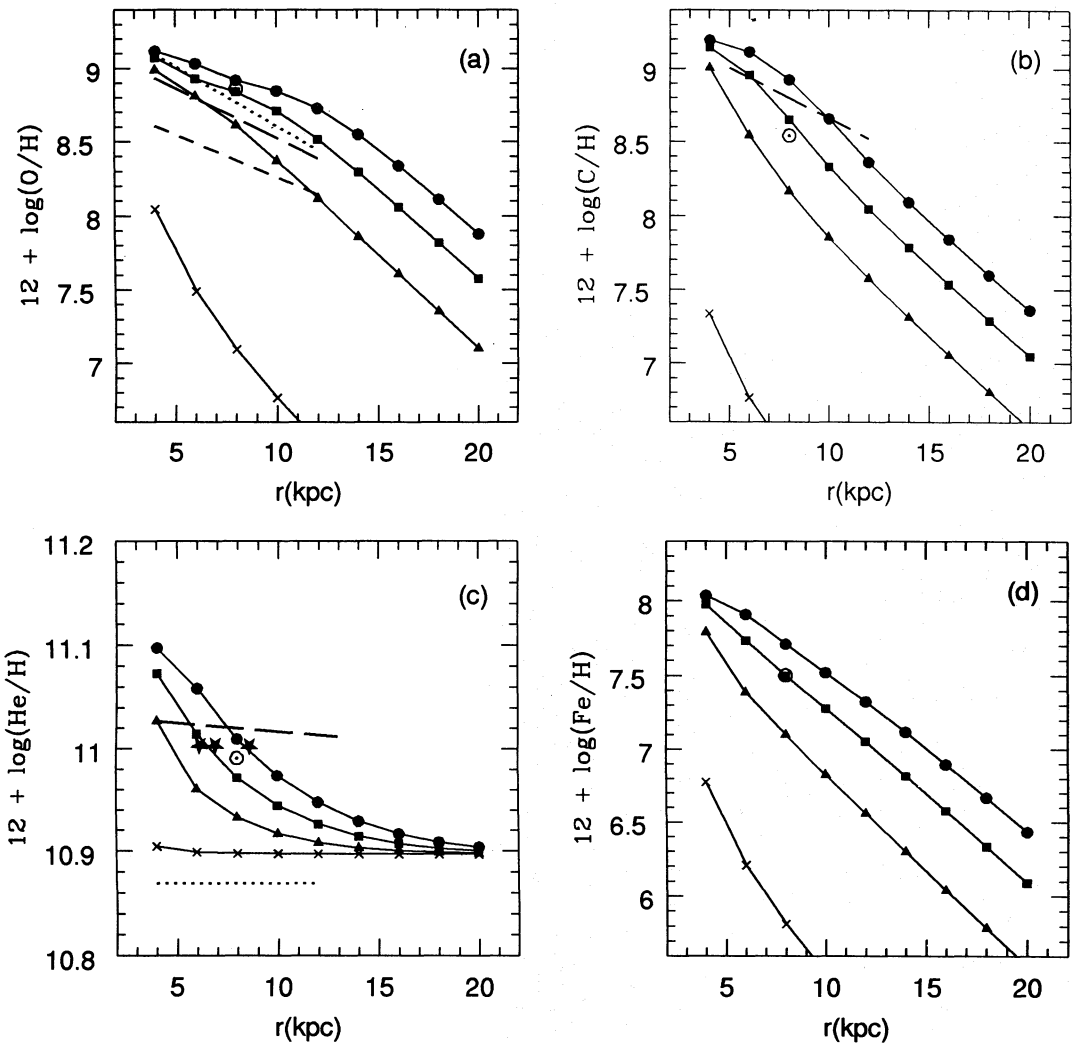

Fig. 5. Evolution of the chemical gradients from the "best model". Radial abundance distributions of oxygen *(a)*, carbon *(b)*, helium *(c)*, and *(d)* iron *(e)* at four different times: 0.5, 4.5, 8.5 and 13 Gyr (*crosses, triangles, squares,* and *circles*, respectively). *Dotted lines:* Observed gradients from H II regions of Shaver et al. (1983). *Long-dashed lines:* Observed gradients from PN II of Maciel & Köppen (1994) for oxygen and of Maciel & Chiappini (1994) for carbon. *Short-dashed lines:* Observed gradients from PN III Maciel & Köppen (1994) for oxygen. *Starred dot:* He abundances from Peimbert, Torres-Peimbert, & Ruiz (1992). The ⊙ symbol marks the solar abundances of Grevesse & Noels (1993).

lution, gives enough gas to inner parts during the second half of the evolution to explain the increase in $\dot{\sigma}_{inf}$ and SFR observed in 3 kpc $< r <$ 8 kpc (Clarke 1989). It is not clear how early outflows and late inflows at different radii would affect the derived O/H(r) distributions from our models but could actually improve the agreement of our modeling with observations, in particular the time-evolution of the gradients.

4. CONCLUSIONS

This work has explored chemical models in which the galactic disk sets up only from primordial infall. Adopting the stellar yields from Maeder (1992) which are strongly dependent on metallicity, the modeling has considered different infall laws, different dependencies of the SFR with the gas and total surface mass densities, and either a constant and homogeneous IMF or a a metal-dependent IMF.

Without appealing for radial flows, models with radially constant infall time-scales and SFR $\propto \sigma_{gas}$ produce no chemical gradients. Models with faster infall towards the center coupled with stronger-than-linear dependencies of the SFR with σ_{gas} predict negative steeper chemical gradients derived from the faster gas consumption in the central zones.

The predicted strength and evolution of the chem-

ical gradients result from the combined effects of the adopted infall-law, SFR, IMF, and the properties of the stellar yields. The main conclusions from this investigation can be summarized as follows:

1. Within $\sim$ 10 kpc, the adopted scale-length for the total surface mass density has little influence on the shape of the inner gradients, but reflects strongly on the slope of the outer gradients. Models with R = 3 kpc reproduce well the present $\sigma_{gas}(r)$ and $\Psi(r)/\Psi_{\odot}$ at all radii, but models with $R \geq 5$ kpc predict distributions that are too flat beyond 10 kpc.

2. Models with a constant and uniform IMF and a SFR $\propto \sigma_{gas}^{x}\sigma_{tot}^{x-1}$ with $1 \leq x \leq 2$ are such that: a) The chemical history of the solar neighborhood is well reproduced. b) A SFR more efficient than $\propto \sigma_{gas}$ (i.e., $x > 1$) is required to obtain an O/H gradient as steep as observed in the galactic disk. c) Rising from unity the x-exponent of the SFR makes the derived O/H(r) distribution to change from concave to convex within $\sim$ 10 kpc, and from flat to convex in the outer zones. These stronger-than-linear SFR dependences on σ_{gas} shift the maximum of the present σ_{gas}(r) distribution towards higher radii, and delay slightly the early ISM enrichment ($\leq$ 1 Gyr with x up to x = 2). d) The strong drop with metallicity of Maeder's oxygen yields, and the constraints from the observed present-day distribution of $\sigma_{gas}/\sigma_{tot}$, prevent these models to completely reproduce at all radii the O/H abundances derived from H II regions.

3. In particular, the model with a SFR = $0.019\,\sigma_{gas}^{1.4}\,\sigma_{tot}^{0.4}\,M_{\odot}$ pc^{-2} Gyr^{-1} (x = 1.4 and a constant and homogeneous IMF), reproduces best most of the observational constraints with the following caveats: a) The predicted O/H(r) profile is consistent with the observed distribution from H II regions, but the model overestimates O/H by $\sim$ 0.2 dex and its oxygen distribution shows too much of a convex behavior. b) Although its present-day O/H(r) distribution is consistent with the observations, this model predicts that the chemical gradients of the heavy elements flatten up with time in contradiction with the observed trend of steepening gradients (below). c) Similarly to models with other x-exponents ($1 < x < 2$), the x = 1.4 model requires maximum gas consumption within the solar ring, and the predicted present-day $\sigma_{gas}(r)$ drops below the observational estimates in the inner zones ($r < 6$ kpc).

4. The chemical gradients of our models evolve with time. The different strengths and evolutions of the radial distribution of the different chemical species are caused mainly by the late contribution of low mass stars, by the strong metallicity sensitivity of the yields from massive stars, and by the primordial composition of the infall: a) Since in our modeling the disk sets up only from primordial infall, the initial He/H gradient is flat. On the other hand, the infall law determines the initial SFR radial distribution which in turn implants its shape to the abundance distributions of the heavier elements at early times. b) Later on, the C/H, O/H, and Fe/H gradients evolve reflecting the history of the SFR radial distribution and the relative rates at which the different chemical species saturate their ISM abundance. c) The abundance saturation is reached first at the inner zones since the infall is stronger and gets consumed faster towards the center. Reaching of the maximum abundance at the center causes the modeled radial distributions of the heavy elements to flatten up with time, since the outer ISM is still being enriched far from saturation through the lower SFR of the outer parts of the disk. d) Unlike the case of heavier atoms, the primordial infall strongly dilutes the He enrichment from the stellar populations, maintaining an almost flat He/H gradient through the whole evolution. The gradient actually steepens a little with time due to a small and slow rise in He/H towards the center.

5. An IMF in which the relative number of very low mass stars decreases with metallicity produces a better match to the observed present-day O/H radial distribution from H II regions (specially within 10 kpc) and can help to reproduce the trend of steepening gradients with time. Unfortunately, this kind of IMF fails to reproduce the early chemical enrichment in the solar neighborhood.

In conclusion, no simple model of this kind can match at once all of the observational constraints set up by: 1) the bimodal behavior of the oxygen abundance distribution from H II regions, steeper towards the galactic center and practically flat beyond 12 kpc; 2) the present-day radial distribution of σ_{gas} and σ_{tot}; 3) a gradient evolution to steeper values; and 4) the early chemical history of the solar neighborhood.

The next paper of the series (Carigi & Peimbert 1997) explores model improvements and other possible scenarios that influence the chemical evolution of the Galaxy, considering in particular: a) a more complex modeling of the Galaxy formation that includes pre-enriched infall into the disk from a previously evolved halo ; b) the use of yields of Woosley & Weaver (1995), which are not as dependent on metallicity as Maeder's yields; c) other IMF dependences on metallicity ; and d) radial gas flows of the type suggested by Clarke (1989).

The author acknowledges useful suggestions and careful reading of the manuscript from M. Peimbert and J. González.

APPENDIX

From models based on essentially the same code used in this work, Carigi et al. (1995, hereafter CCPS) demonstrated the need for an IMF that changes with metallicity in order to match the

present-day oxygen abundance and the gas mass fraction in a typical irregular galaxy. In particular, the authors take as a reference a KTG IMF (Kroupa, Tout, & Gilmore 1993):

$$\Phi(m) = \begin{cases} 0.510\ m^{-1.3} & \text{for } 0.01 \leq m < 0.5 \\ 0.273\ m^{-2.2} & \text{for } 0.5 \leq m < 1.0 \\ 0.273\ m^{-2.7} & \text{for } 1.0 \leq m < 120.0 \end{cases}, \quad (4)$$

and vary the slope of its low-mass end to define a modified IMF as

$$\Upsilon(m) = D \begin{cases} (0.5^{y-2.2}) m^{-y} & \text{for } 0.01 \leq m < 0.5 \\ m^{-2.2} & \text{for } 0.5 \leq m < 1.0 \\ m^{-2.7} & \text{for } 1.0 \leq m < 120.0 \end{cases}, \quad (5)$$

with D such that $\int_{0.01}^{120} m\Upsilon dm \equiv 1$, and a slope y which varies with metallicity. A factor that measures the number of stars that contributes to the ISM enrichment relative to the KTG IMF can be defined as

$$\varrho = \frac{\int_{0.05}^{120} m\Phi(m)dm}{\int_{0.05}^{120} m\Upsilon(m)dm} . \quad (6)$$

A consistent dependence of ϱ (or equivalently y) with metallicity can in principle be derived from the modeling of systems with different present-day abundances. In particular, CCPS evolved a couple of closed-box models with different y exponents (held constant during the evolution of ~ 10 Gyr) and, taking $\varrho(X_{\rm O}) = 1$ for the solar neighborhood, one derives the $\varrho(X_{\rm O}) \propto X_{\rm O}^{-1}$ for the set of three final oxygen abundances by mass $X_{\rm O}$. But before their use in models that account for the IMF variations with abundance (i.e., $y \neq const$ during the evolution), the so derived $\varrho(X_{\rm O})$ factors have to be interpreted strictly as some kind of time average over the evolution:

$$\langle\varrho\rangle(X_{\rm O}) = \frac{\int_0^{X_{\rm O}} \varrho(x_{\rm O}) w(x_{\rm O}) dx_{\rm O}}{\int_0^{X_{\rm O}} w(x_{\rm O}) dx_{\rm O}} , \quad (7)$$

where the weighing function $w(x_{\rm O})$ is an a-priori unknown factor driven by the details of the modeling of the chemical evolution.

In this work, we completed the CCPS mapping of $\langle\varrho\rangle(X_{\rm O})$ with more closed-box and infall models, and probed other gas consumptions as well as different yields, to derive a consistent $\varrho(x_{\rm O})$ from eq. (7).

Since the chemical composition of the solar vicinity is very well known, it provided us with a very good test to probe the influences of almost every ingredient in the chemical models. After trying without success many simple analytical, continuous and bounded forms for $\varrho(x_{\rm O})$ in the solar neighborhood, that apply over a considerable range in oxygen abundance, we arrived at the following expression from which we obtain the best match for the solar C/O abundance after 8.5 Gyr

$$\varrho(x_{\rm O}) = \begin{cases} a\ (x_{\rm O}/10^{-3})^2 + b & \text{for } x_{\rm O} \leq x_{\rm Ol} \\ 6.0\ (x_{\rm O}/10^{-3})^{-1.5} & \text{for } x_{\rm Ol} < 4.2 \times 10^{-3} \\ 0.7 & \text{otherwise,} \end{cases} \quad (8)$$

where a and b are chosen such that the function and its first derivative are continuous at $x_{\rm Ol} = 1.5 \times 10^{-3}$. The integral of eq. (8) fairly matches the values mapped in detail $\langle\varrho\rangle(X_{\rm O})$.

In this work, we used implicitly the above expression for $\varrho(x_{\rm O})$ as the metallicity dependency of the modified $\Upsilon(m)$ initial mass function (IMF($x_{\rm O}$) in the text).

REFERENCES

Abia, C., Canal, R., & Isern, J. 1991, ApJ, 366, 198
Bessell, M.S., Sutherland, R.S., & Ruan, K. 1991, ApJ, 383, L71
Carigi, L. 1994, ApJ, 424, 181
Carigi, L., Colín, P., Peimbert, M., & Sarmiento, A. 1995, ApJ, 445, 98 (CCPS)
Carigi, L., & Peimbert, M. 1997, in preparation
Chiappini, C., Matteucci, F., & Gratton, R. 1996, ApJ, submitted
Clegg, R.E.S., Lambert, D.L., & Tomkin, J. 1981, ApJ, 250, 262
Clarke, C.J. 1989, MNRAS, 238, 283
Dame, T.M. 1993, in Back to the Galaxy, ed. S. Holt & F. Verter (AIP), 267
Díaz, A.I. 1989, in Evolutionary Phenomena in Galaxies, ed. J.E. Beckman & B.E.J. Pagel (Cambridge: Cambridge Univ. Press), 377
Doane, J.S., & Mathews, W.G. 1993, ApJ, 419, 573
Edmunds, M.G., & Roy, J.R. 1993, MNRAS, 261, L17
Edvardsson, B., Andersen, J., Gustafsson, B., Lambert, D.L., Nissen, P.E., & Tomkin, J. 1993, A&A, 275, 101
Esteban, C., & Peimbert, M. 1995, in The Fifth Mexico-Texas Conference on Astrophysics: Gaseous Nebulae and Star Formation, ed. M. Peña & S. Kurtz, RevMexAASC, 3, 133
Faúndez-Abans, M., & Maciel, W.J. 1986, A&A, 158, 228
Ferrini, F., Mollá, M., Pardi, M.C., & Díaz, A.I. 1994, ApJ, 427, 745
Franco, J., & Shore, S.N. 1984, ApJ, 285, 813
Gerhard, O.E. 1994, in Panchromatic View of Galaxies, ed. G. Hensler, Ch. Theis, & J.S. Gallagher (Singapore: Frontiers), 417
Gilmore, G. 1989, in The Milky Way as a Galaxy, ed. R. Buser & I. King (Geneva: Geneva Observatory), 36
Giovagnoli, A., & Tosi, M. 1995, MNRAS, 273, 499
Grevesse, N., & Noels, A. 1993, in Origin and Evolution of the Elements, ed. N. Prantzos, E. Vangioni-Flam, & M. Cassé (Cambridge: Cambridge Univ. Press), 14
Kilian-Montenbruck, J., Gehren, T., & Nissen P.E. 1994, A&A, 291, 757
Kroupa, P., Tout, C.A., & Gilmore, G. 1993, MNRAS, 262, 545 (KTG)

Kuijken, K., & Gilmore, G. 1989, MNRAS, 239, 605
_____. 1991, ApJ, 367, L9
Lacey, C.G., & Fall, S.M. 1985, ApJ, 290, 154
Maciel, W.J., & Chiappini, C. 1994, Ap&SS, 219, 231
Maciel, W.J., & Köppen, J. 1994, A&A, 282, 436
Maeder, A. 1992, A&A, 264, 105
Matteucci, F., & François, P. 1989, MNRAS, 239, 885
Matteucci, F., Franco, J., François, P., & Treyer, A. 1989, RevMexAA, 18, 145 (MFFT)
Méra, M., Chabrier G., & Barafee I. 1996, ApJ, 459, L87
Mirabel, I.F. 1989, in IAU Colloq. 120, Structure and Dynamics of the Interstellar Medium, ed. G. Tenorio-Tagle, M. Moles, & J. Melnick (Berlin: Springer-Verlag), 396
Peimbert, M. 1979, in The Large Scale Characteristics of the Galaxy, ed. W.B. Burton (Dordrecht: Reidel), 307
_____. 1995 in Highlights in Astronomy, Vol. 10, ed I. Appenzeller (Dordrecht: Kluwer), 486
Peimbert, M., Torres-Peimbert, S., & Ruiz, M.T. 1992, RevMexAA, 24, 155
Prantzos, N., & Aubert, O. 1995, A&A, 302, 69
Rana, N.C. 1991, ARA&A, 29, 129
Rana, N.C. & Basu, S. 1992, A&A, 265, 499
Richer, H.B. et al. 1995, ApJ, 451, L17
Rieke, G.H., Loken, K., Rieke M.J., & Tamblyn, P. 1993, ApJ, 412, 99
Rocha-Pinto, H.J., & Maciel, W.J. 1996, MNRAS, 279, 447
Scalo, J.M. 1986, Fund. Cosm. Phys., 2, 1
Shaver, P.A., McGee, R.X., Newton, L.M., Danks, A.C., & Pottasch, S.R. 1983, MNRAS, 204, 53
Silk, J. 1995, ApJ, 438, L41
Tosi, M. 1988 A&A, 197, 33
_____. 1996, ASP Conf. Ser., Vol. 98, From Stars to Galaxies: The Impact of Stellar Physics on Galaxy Evolution, ed. C. Leitherer, U.F. von-Alvensleben, & J. Huchra, 299
Vílchez, J.M., & Esteban, C. 1996, MNRAS, 280, 720
Weaver, T.A., & Woosley, S.E. 1993, Phys. Reports, 227, 65
Woosley, S.E., & Weaver, T.A. 1995, ApJS 101, 181
Zaritsky, D., Kennicutt, R.C., & Huchra, J.P. 1994, ApJ, 420, 87
Zinnecker, H. 1994, in Panchromatic View of Galaxies, ed. G. Hensler, Ch. Theis, & J.S. Gallagher (Singapore: Frontières), 334

Leticia Carigi: Instituto de Astronomía, UNAM, Apartado Postal 70-264, 04510 México D.F., México. (carigi@astroscu.unam.mx).